Fluid-structure interactions simulation to explain thermal sleeve wear mechanism in a pressurized water reactor

Clément VIRON[1], Hemish MISTRY[2], Daniele VIVALDI[1], Antoine LEJOSNE[1], Angel PAPUKCHIEV[2]

[1] Autorité de Sûreté Nucléaire et de Radioprotection (ASNR), Fontenay-aux-Roses, France
[2] Gesellschaft für Anlagen- und Reaktorsicherheit (GRS) gGmbH, Garching, Germany

Abstract: Thermal sleeve wear has occurred in PWRs. Despite the safety concerns associated with thermal sleeves, the numerical analysis of the associated Fluid-Structure Interaction (FSI) mechanisms is rather recent. A study based on CFD to simulate the global primary flow in the upper head is presented in this paper and seems to be a promising way to predict flow-induced loads on the thermal sleeves. The sleeves located in the central region of the upper head are found to be subjected to the highest radial force fluctuations, which appears consistent with the observed failures in PWRs. To assess numerical approaches for future FSI simulations of thermal sleeves, FSI simulations of two experimental tests in axial and cross flow are also presented in this paper.

1 THERMAL SLEEVES OVERVIEW AND SAFETY ISSUES

1.1 Design and use

In PWRs, thermal sleeves are, e.g., located inside the Control Rod Drive Mechanism (CRDM) adapter (the penetration through the Reactor Pressure Vessel (RPV) upper head, **Figure 1**).

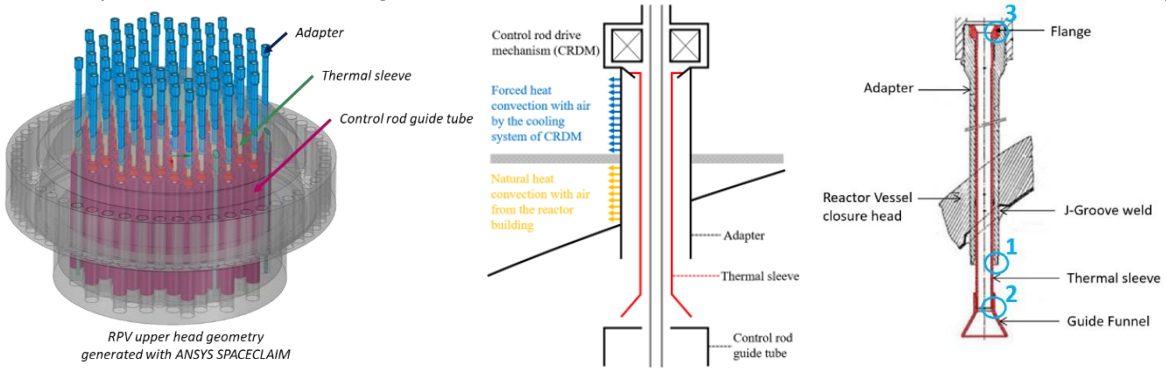

Figure 1 – Left: RPV upper head geometry (thermal sleeves in green and red). Center: Schematic of the thermal sleeve inside the CRDM adapter. Right: Schematic of the thermal sleeve with its different parts.

Thermal sleeves have the following functions: they guide and allow to center the rod cluster control assembly (RCCA) drive rods into the reactor pressure vessel (RPV) head penetrations; during SCRAM, the upward coolant flow lifts them, increasing the water flowing area, thus reducing the pressure drop and the RCCA dropping time; during RCCA drive rod stepping up, they avoid thermal shocks on the adapter welding on the RPV head by channeling the cooled water from the CRDM inside them; they limit the temperature fluctuations in the adapter region.

As thermal sleeves move almost freely inside CRDM adapters and are subjected to strong and fluctuating coolant flows, they are affected by fatigue and wear.

1.2 International feedback on thermal sleeves

In the U.S., the first thermal sleeve wear issues were reported in 2007 on several Westinghouse reactors [1]. They were located on one of the 3 locations on **Figure 1**. In 2014,

a thermal sleeve fell from the reactor vessel head during an inspection: it turned out that the flange had worn through and separated.
In France in 2017, during normal operation of Saint-Alban and Belleville NPPs Units 2, a central RCCA has been blocked [2]. Inspection found a ring of steel that was the detached flange of the thermal sleeve, impeding the motion of the rod. In 2018, a similar problem was detected at Nogent-sur-Seine NPP Unit 1 during a RCCA drop time test [3][4]. General inspection showed that thermal sleeve wear was observed in various French PWRs. CFD studies has been performed for the assessment [5][6][7][8] and are presented in [11].
In the UK, a thermal sleeve was found detached and resting on the upper internals after removing the RPV upper head at Sizewell B [12].

1.3 Safety aspects related to thermal sleeve wear

Deterioration or breaking of thermal sleeves can lead to safety issues such as: a delayed RCCA drop time (which can affect safety functions); a decreased negative reactivity insertion in case of SCRAM with blocked RCCA control rods; the generation of foreign objects from worn thermal sleeve in the primary circuit that can lead to damages on RPV internals, steam generators U-tubes or coolant pumps; a risk of damages and maintenance in case of its fall when the RPV upper head is lifted; stronger thermal demands on the control rod drive mechanism (CRDM) adapter welds with a breaking risk that can lead to a loss-of-coolant accident (LOCA) on RPV upper head and/or rod ejection transient.

2. THERMAL SLEEVE FLANGE WEAR MECHANISM

Flange wear is caused by thermal sleeves rotational movements, resulting from fluid-induced excitation mechanisms. PWRs featuring temperature-cold head configuration may be more susceptible to thermal sleeve wear [13]. In this configuration, coolant from the downcomer enters the RPV upper head through bypass nozzles, merges at its top, turns around and goes down toward the control rod guide tubes top opening, where it is evacuated to the upper plenum.

2.1 CFD simulation of the flow inside the RPV upper head

CFD simulations of the nominal flow inside the RPV upper head were performed with ANSYS CFX 19.1. Boundary conditions are located at the bypass nozzles allowing the coolant to enter the upper head from the downcomer, and at the bottom end of each upper control rod guide tube (i.e. at the top support plate). An imposed flow rate exiting the upper control rod guide tubes was first used as boundary condition, together with a fixed imposed pressure at the bypass nozzles. The pressure drop obtained with such boundary conditions was then employed to fix the pressure on both boundaries of the domain, as this allows for different flow rates in each nozzle and control rod guide tube. Sensitivity to the mesh refinement in the near-wall region was performed. The final converged mesh consists of around 19 M cells, both tetrahedral and hexahedral. The simulations use the URANS k-ω-SST model and the time step is fixed to 5.10^{-3} s.
Numerical results show high velocities near the central upper head internals, induced by the flow turnaround. The central thermal sleeves are surrounded by the highest flow velocity, as observed in **Figure 2**.

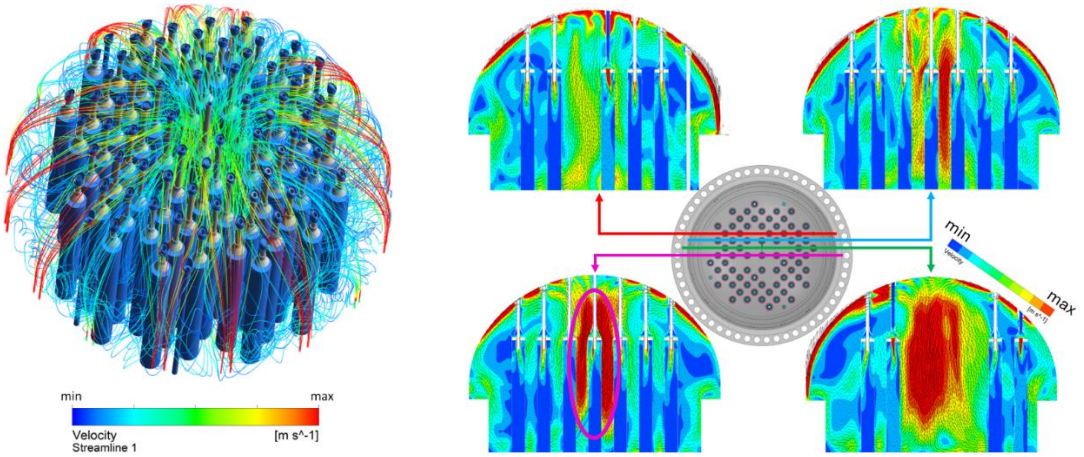

Figure 2 – Velocity streamlines (left) and contours (right) of the flow inside the RPV upper head. Scales are not quantified purposely.

2.2 Evaluation of the hydraulic loads on thermal sleeve during normal operation

Hydraulic loads on thermal sleeves were computed based on the CFD results: the highest ones and the strongest fluctuations are located on the central and the two first rings of thermal sleeves, as shown in **Figure 3** (left). These thermal sleeves tend to be pushed down, whereas peripheral ones tend to be lifted by the flow.

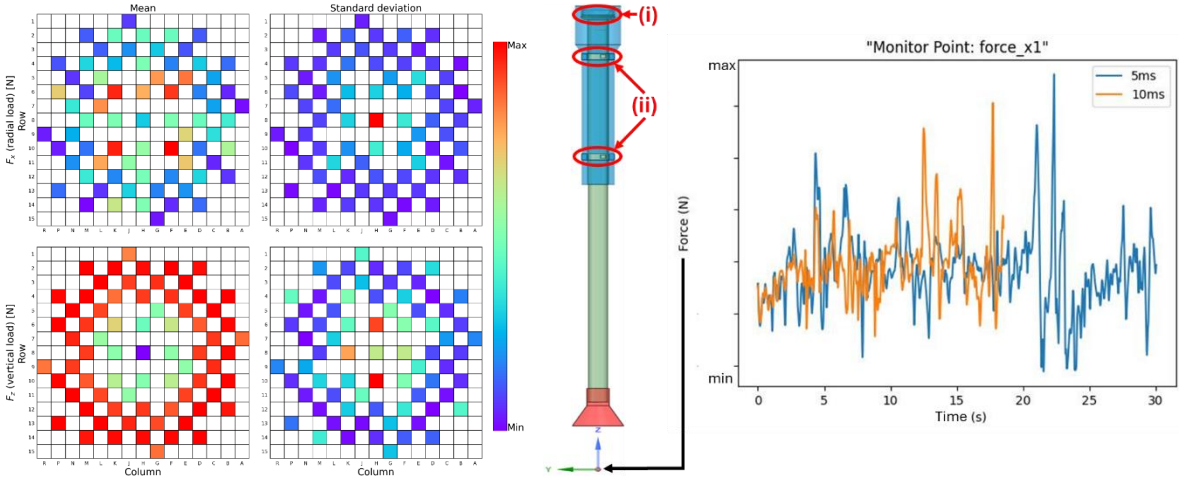

Figure 3 – Left: Hydraulics loads (top: radial and bottom: vertical) computed for each thermal sleeve (left: mean value and right: temporal standard deviation). Center: Mechanical model of the thermal sleeve inside its adapter, with its identified zones of friction connections. Right: Hydraulics loads evaluated by the CFD simulation and applied at the mechanical model at the same point. Scales are not quantified purposely.

2.3 Mechanical analysis of the thermal sleeve behavior inside its CRDM adapter

The calculated hydraulic loads were then used as an input for a mechanical analysis of the thermal sleeve inside its CRDM adapter. A one-way approach was retained, *i.e.* the effect of the thermal sleeve motion on the coolant flow was not considered. As the thermal sleeve is not locked onto the adapter, friction connections are defined (i) at the top between the adapter flange and the thermal sleeve ledge and (ii) around the centering pins, as shown on **Figure 3** (center). Mechanical stresses and displacements were computed and show that hydraulic loads induce a small, but fluctuating motion of the thermal sleeve inside the adapter which can explain the wear at the interfaces.

Archard wear equation [14] was used to evaluate the wear speed of the central thermal sleeve during the CFD transient time. Considering 40 years of constant service and mechanical properties of 304L stainless steel [15], 12 mm wear is calculated, which corresponds to approximately half the flange height.

3. ASSESSMENT OF FSI SIMULATIONS FOR THERMAL SLEEVES

With the goal of performing future FSI numerical analysis of thermal sleeves, preliminary numerical tests have been carried out on experimental configurations designed to study FSI. Two configurations were analyzed: a flexible cylinder subjected to water cross-flow and a cantilever beam subjected to water axial flow. They represent the two extreme flow configurations seen by a thermal sleeve.

3.1 The AMOVI experiment

Experimental results from the CEA's hydraulic loop AMOVI were used as benchmark for cross-flow FSI simulation assessment [16]. The analysis presented in this paper was performed within the European GO-VIKING project [17] and considers a test with one flexible tube exposed to a volumetric flow rate of 2.9 l/s at 25°C (Re~40000), see **Figure 4** (left). The tube vibrates primarily in the lift direction (*i.e.* perpendicular to the main flow), with a natural frequency f_n = 27.5 Hz and a damping ratio of ξ_n = 0.064, in air.

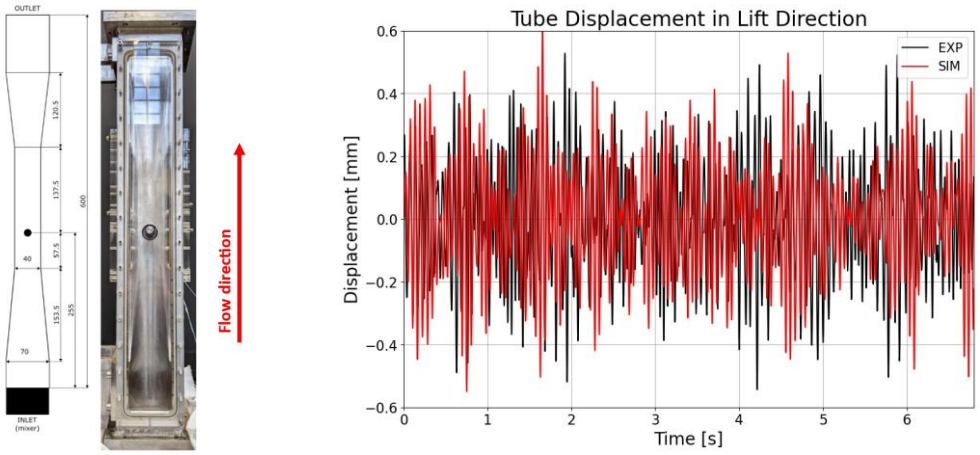

Figure 4 – Left: AMOVI test section with a single flexible tube. Right: Measured and calculated tube displacement.

3.1.1 Numerical FSI approach

Regarding the simulation of the structure, the AMOVI tube is rigid (*i.e.*, it does not deform), one of its edges is free to vibrate and the other is attached to a deforming blade system (in turn attached to test section wall): this results in a 1-degree of freedom rotational motion along one axis (the flexible direction of the blade). This motion was therefore simulated through a rigid body model, the motion of which is dictated by the fluid forces and torques acting on it [18].

For the flow simulation, a URANS approach based on the Reynolds-stress Stress-Omega model was used. A high-resolution advection scheme and a second order backward Euler scheme were used. The time step was fixed equal to 2.10^{-4} s. The coupling approach was based on an implicit two-way coupling scheme.

3.1.2 Results

Figure 4 (right) compares the calculated and the experimental tube displacements. A time averaged tube displacement of 0.179 mm is calculated, which agrees well with the 0.19 mm measured experimentally. The measured vortex-shedding frequency of 15 Hz is slightly overpredicted in the simulation by just 1 Hz.

3.2 THE CANTILEVER BEAM EXPERIMENT

The experimental tests performed by the University of Manchester on a cantilever beam subjected to axial water flow [19] are used as benchmark for FSI simulations in axial flow. The experimental configuration (see **Figure 5** (a)) consists of a 1 m long vertical, cylindrical beam, with a diameter of 11 mm. Water flows upward inside a cylindrical section of 22 mm diameter, surrounding the beam: after a free region, the flow impacts the free tip of the beam and then continues inside the annulus downstream of the tip (see **Figure 5** (b)). The beam natural frequency and damping ratio in water are 3.7 Hz and 0.014, respectively. The water velocity is 1.03 m.s^{-1} in the free section, corresponding to Re=16000. The work presented in this paper is also part of the European GO-VIKING project [17].

3.2.1 Numerical FSI approach

All simulations were run with code_Saturne v7. Regarding the simulation of the structure, the beam was modeled through a 1-D finite-element Euler-Bernoulli approach, implemented in code_Saturne. A discretization on 30 nodes was used.

The water flow was simulated following various approaches: different URANS models and the DDES hybrid URANS/LES one. Depending on the specific turbulence approach, a SOLU or central advection scheme was used, with a first or second order time scheme.

The fluid-structure coupling approach was 2-way explicit, meaning that the fluid and structure are coupled at each time step, however without inner sub-iterations.

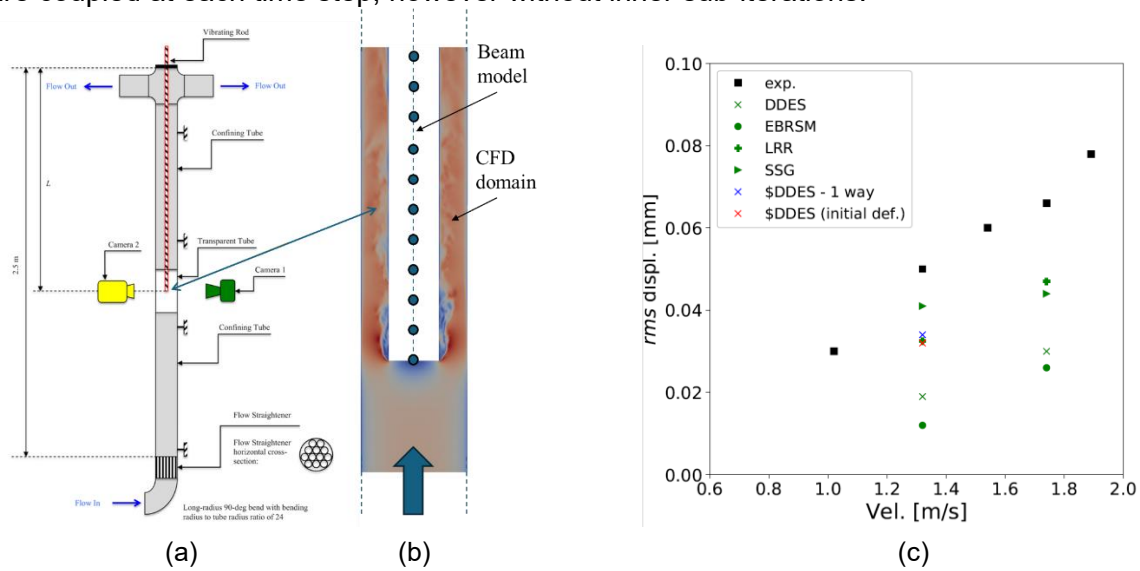

(a) (b) (c)

Figure 5 – Cantilever beam benchmark: (a) schematics of the experimental configuration, (b) contour of water velocity around the free tip of the beam, (c) experimental and numerical rms displacement.

3.2.2 Results

The results were first validated in terms of calculated natural frequency (in air and water) and damping. The calculated displacements of the free tip of the beam are compared to the ones

measured experimentally in **Figure 5** (c). We note that the numerical results depend largely on the turbulence approach employed. Unexpectedly, lower resolution approaches such as RSM-SSG and RSM-LRR models calculate higher vibration amplitudes than the higher resolution approaches EB-RSM and DDES. This suggests that further analyses are required to understand the details of the FSI mechanisms predicted by the different numerical approaches.

CONCLUSION

Decoupled CFD and structural simulation of the thermal sleeves inside a PWR RPV upper head were performed. First results show that the coolant flow induces strong loads on central thermal sleeves, leading to displacements, structural stresses and eventually to material wear. Results are promising, but FSI analyses are required to deepen the understanding of the underlying mechanisms. For this reason, preliminary benchmark FSI simulations were performed employing available results on two European GO-VIKING project experiments, AMOVI and a cantilever beam, for flow-induced vibrations in cross and axial flows, respectively. The numerical results agree with the experimental measurements, however further analyses to understand specific turbulence model behaviors are necessary. Still, the overall qualitative agreement of simulations with test data supports the conclusion that the application of FSI analyses to actual safety concerns such as for the thermal sleeves is a valid approach.

REFERENCES

[1] D. Rudland *et al.*, “Predicting the impact of CRDM thermal sleeve wear in Westinghouse pressurized water reactors”, Transactions, SMiRT-25, Charlotte, NC, USA, August 4-9, 2019.
[2] Incident de niveau 1 concernant un risque de blocage de grappes de commande [...] - 03/09/2021 - ASN
[3] Risque de blocage de grappes de commande des réacteurs de 1300 MWe - 03/09/2021 - ASN
[4] “Méthodologie et critère d'usure des manchettes thermiques des adaptateurs de couvercle de cuve”, IRSN/2018-00281, October 19, 2018.
[5] “Réacteur électronucléaire n°1 du CNPE de Nogent-sur-Seine – Retrait de manchettes thermiques sur les positions non grappées du cercle 3 du couvercle de cuve pour une durée de 2 cycles”, IRSN/2019-00105, May 16, 2019.
[6] “Réacteur électronucléaire n°1 de la centrale nucléaire de Nogent – Autorisation de modification notable – Retrait de manchettes thermiques sur les positions non grappées du cercle 3 du couvercle de cuve pour une durée de deux cycles”, CODEP-DCN-2019-023102, May 24, 2019.
[7] “Réacteurs électronucléaires de 1300 Mwe – Retrait de manchettes thermiques sur les positions non grappées du cercle 3 des couvercles de cuve”, IRSN/2020-00079, May 26, 2020.
[8] “Réacteurs électronucléaires de 1300 Mwe – EDF – Autorisation de modification notable – Retrait de manchettes thermiques sur les positions non grappées du cercle 3 des couvercles de cuve”, CODEP-DCN-2020-028999, June 14, 2020.
[9] “Mise en place d’un dispositif en partie supérieur des guides de grappes afin de limiter l’usure des manchettes thermiques”, IRSN/2021-00091, May 31, 2021.
[10] Public information by Framatome on thermal sleeves wear.
[11] P. Ruyer, J. Roy, C. Viron, and C. Heib, “Using CFD in the frame of safety studies - some IRSN experiences”, in Proceedings of CFD4NRS-8, Paris-Saclay, France, November 2020.
[12] “Site Report for Sizewell B – Report for period 1 July – 30 September 2021”, ONR-DOC-TEMP-008 (Issue 9.2), © Office for Nuclear Regulation (ONR), 2022.

[13] "Technical assessment of potential control rod drive mechanism thermal sleeve failure", NRC ML18249A107 - CRDM Thermal Sleeve LIC-504 - rev 2., 2018.
[14] J.F. Archard, "Contact and Rubbing of Flat Surfaces", J. of Applied Physics, 24, 981-988, 1953.
[15] J.M. Challen *et al.*, "Prediction of Archard's wear coefficient for metallic sliding friction assuming a low cycle fatigue wear mechanism", Wear, Volume 111, Issue 3, Pages 275-288, 1986.
[16] D. Panunzio *et al.*, "Experimental investigation of cross-flow fluidelastic instability for rotated triangular tube bundles subjected to single-phase and two-phase transverse flows", 12th International Conference on Fluid-Induced Vibration, July 5-8, 2022, Paris-Saclay, France.
[17] A. Papukchiev, K. Zwijsen, D. Vivaldi, H. Hadžić, S. Benhamadouche, W. Benguigui and P. Planquart "The European GO-VIKING Project on Flow-Induced Vibrations: Overview and Current Status", Kerntechnik journal, published online March 15, 2024, https://doi.org/10.1515/kern-2023-0126.
[18] A. Papukchiev, H. Mistry, and J. Herb, "Flow-induced vibrations in nuclear steam generators: simulation of the AMOVI experiment with different FSI approaches", NUTHOS-14 Conference, August 25-28, 2024, Vancouver, Canada.
[19] A. Cioncolini et al., "Axial-flow-induced vibration experiments on cantilevered rods for nuclear reactor applications", Nucl. Eng. and Des., 338, 2018.